

# Evolution of the electronic structure from electron-doped to hole-doped states in the two-dimensional Mott-Hubbard system $\text{La}_{1.17-x}\text{Pb}_x\text{VS}_{3.17}$

A. Ino,<sup>1,\*</sup> T. Okane,<sup>1</sup> S.-I. Fujimori,<sup>1</sup> A. Fujimori,<sup>1,2</sup> T. Mizokawa,<sup>2</sup> Y. Yasui,<sup>3</sup> T. Nishikawa,<sup>3</sup> and M. Sato<sup>3</sup>

<sup>1</sup>*Synchrotron Radiation Research Center, Japan Atomic Energy Research Institute, Mikazuki, Hyogo 679-5148, Japan*

<sup>2</sup>*Department of Complexity Science and Engineering, University of Tokyo, Bunkyo-ku, Tokyo 113-0033, Japan*

<sup>3</sup>*Department of Physics, Nagoya University, Chikusa-ku, Nagoya 464-8602, Japan*

The filling-controlled metal-insulator transition (MIT) in a two-dimensional Mott-Hubbard system  $\text{La}_{1.17-x}\text{Pb}_x\text{VS}_{3.17}$  has been studied by photoemission spectroscopy. With Pb substitution  $x$ , chemical potential  $\mu$  abruptly jumps by  $\sim 0.07$  eV between  $x = 0.15$  and  $0.17$ , indicating that a charge gap is opened at  $x \simeq 0.16$  in agreement with the Mott insulating state of the  $d^2$  configuration. When holes or electrons are doped into the Mott insulator of  $x \simeq 0.16$ , the gap is filled and the photoemission spectral weight at  $\mu$ ,  $\rho(\mu)$ , gradually increases in a similar way to the electronic specific heat coefficient, although the spectral weight remains depressed around  $\mu$  compared to that expected for a normal metal, showing a pseudogap behavior in the metallic samples. The observed behavior of  $\rho(\mu) \rightarrow 0$  for  $x \rightarrow 0.16$  is contrasted with the usual picture that the electron effective mass of the Fermi-liquid system is enhanced towards the metal-insulator boundary. With increasing temperature, the gap or the pseudogap is rapidly filled up, and the spectra at  $T = 300$  K appears to be almost those of a normal metal. Near the metal-insulator boundary, the spectra around  $\mu$  are consistent with the formation of a Coulomb gap, suggesting the influence of long-range Coulomb interaction under the structural disorder intrinsic to this system.

PACS numbers: 71.30.+h, 79.60.-i, 71.27.+a, 71.20.Be, 71.23.-k

## I. INTRODUCTION

For more than a decade, extensive studies have been devoted to clarifying how the electronic structure evolves in filling-controlled metal-insulator transition (MIT) systems in the presence of strong electron correlation,<sup>1</sup> stimulated by the discovery of high- $T_c$  superconductivity in the cuprates. Empirically, many three-dimensional perovskite-type  $3d$ -transition-metal oxides become insulators when the band filling approaches an integer number.<sup>2</sup> For example,  $\text{La}_{1-x}\text{Sr}_x\text{TiO}_3$  shows a filling-controlled MIT at  $x \simeq 0.06$ ; the electron effective mass  $m^*$  is enhanced on approaching the metal-insulator phase boundary from the metallic side.<sup>3,4,5</sup> Simultaneously, the quasiparticle (QP) band at the chemical potential  $\mu$  becomes narrower, and the spectral weight is transferred from the QP band to the lower Hubbard band.<sup>5,6</sup> In a two-dimensional system  $\text{La}_{2-x}\text{Sr}_x\text{CuO}_4$ , on the other hand, the effective mass  $m^*$  decreases towards the metal-insulator phase boundary, a pseudogap in the normal state is formed and eventually evolves into the Mott insulating gap.<sup>7,8</sup> In order to induce the relationship between the dimensionality and the behavior of the electronic states near MIT, it is necessary to study the electronic structure of other two-dimensional filling-controlled systems. In addition, when we discuss the behavior of the filling-controlled MIT, we should also consider the effect of structural disorder, which is inevitably introduced into the system by atom substitution to realize the filling control. Under the influence of disorder in real systems,<sup>9</sup> a small number of doped carriers are necessarily Anderson-localized and thus feel a long-range Coulomb interaction. The above factors intricately involved in the MIT of cor-

related systems should be seriously considered, since a variety of phenomena including high- $T_c$  superconductivity and colossal magnetoresistance appear near the filling-controlled MIT.

Recently, filling control over a very wide doping range encompassing both electron and hole doping has been realized in a two-dimensional “misfit-layer” compound system  $\text{La}_{1.17-x}\text{A}_x\text{VS}_{3.17}$  ( $\text{A} = \text{Sr}$  or  $\text{Pb}$ ).<sup>10,11,12,13</sup> The crystal structure is composed of alternately stacking LaS and  $\text{VS}_2$  layers.<sup>14,15</sup> While the structure of the LaS layer is a distorted rock-salt type, the  $\text{VS}_2$  layer forms a two-dimensional triangular lattice of the V atoms which are octahedrally surrounded by S atoms. Therefore, while the lattice constants of LaS and  $\text{VS}_2$  layers may be commensurate in one direction, they are inevitably incommensurate in the other direction. Remarkably, both electron doping ( $x \lesssim 0.16$ ) and hole doping ( $x \gtrsim 0.16$ ) are possible within the single system, and therefore  $\text{La}_{1.17-x}\text{A}_x\text{VS}_{3.17}$  is an unique system for studying the filling-controlled MIT. According to the electrical resistivity measurement,<sup>10,11,12</sup> the system become most insulating when the substitution  $x$  approaches  $x \simeq 0.16$ , where the triply degenerated  $t_{2g}$  orbitals of V  $3d$  are filled by two electrons. Assuming that the doped hole concentration  $\delta$  is given by  $\delta \equiv x - 0.16$  (and hence that the doped electron concentration is given by  $-\delta \equiv 0.16 - x$ ), the holes and electrons are doped up to  $\delta \simeq 0.19$  and  $-\delta \simeq 0.16$ , respectively. Also the Hall coefficient and thermoelectric power measurements<sup>10,11</sup> have indicated that the carrier density decreases towards the insulating limit  $x \simeq 0.16$  and the carrier changes its sign between  $x < 0.15$  and  $x \geq 0.17$ . Furthermore, those two transport properties are considerably temperature dependent

in a similar way to the high- $T_c$  cuprates. Another similarity to the cuprates is that the low-temperature electronic specific-heat coefficient  $\gamma$  *diminishes* towards the Mott insulating state.<sup>12</sup> In the insulating phase of  $\text{La}_{1.17-x}\text{A}_x\text{VS}_{3.17}$ , a nonmagnetic behavior has been indicated by a nuclear-magnetic-resonance (NMR) study.<sup>13</sup> Lattice distortions in the insulating sample  $x = 0.17$  are suggested by anomalies at  $\sim 280$  K in the temperature dependence of the thermal dilatation and the ultrasound velocity.<sup>12</sup>

In the present study, the electronic structure of  $\text{La}_{1.17-x}\text{Pb}_x\text{VS}_{3.17}$  is systematically studied by means of photoemission spectroscopy. We have investigated the chemical-potential shift with carrier-doping, and the doping and temperature dependence of the density of states (DOS) of the V 3*d* band. We also discuss possible effects of structural disorder under strong electron correlations near the MIT.

## II. EXPERIMENT

Polycrystalline samples of  $\text{La}_{1.17-x}\text{Pb}_x\text{VS}_{3.17}$  ( $x = 0, 0.1, 0.15, 0.17, 0.25, 0.3, \text{ and } 0.35$ ) were prepared by sintering a mixture of  $\text{La}_2\text{S}_3$ , Pb, V, and S powders at 1050 – 1150 °C. X-ray powder-diffraction patterns indicated that single-phase samples were obtained.<sup>10</sup> Details of the sample preparation are described elsewhere.<sup>10,11,12</sup> High-resolution photoemission spectroscopy was performed for the valence band, using a GAMMADATA-SCIENZA SES-2002 hemispherical electron-energy analyzer and a GAMMADATA-SCIENZA VUV-5010 helium discharge lamp. The overall instrumental resolution was 4 meV including the natural width of the excitation source. The base pressure in the spectrometer chamber was about  $3 \times 10^{-10}$  Torr. Clean surfaces were obtained by scraping *in situ* with a diamond file. All the spectra were recorded within 90 and 60 min after scraping at  $T = 14$  K and  $T = 300$  K, respectively, so that the signals of broad spectral features around  $-6$  eV and  $-8$  eV due to surface contamination became inappreciable. Also x-ray photoemission spectroscopy (XPS) and x-ray absorption spectroscopy (XAS) were performed for core levels. The XPS spectra were collected using a double-pass cylindrical-mirror analyzer, using the Mg K  $\alpha$  line ( $h\nu = 1253.6$  eV). The XAS spectra were collected in the total electron yield method using synchrotron radiation at beamline 2 of Photon Factory, High Energy Accelerators Research Organization. The base pressure in the vacuum chamber was in low  $10^{-10}$  Torr range, and the spectra were taken at liquid-nitrogen temperature  $T = 77$  K and at  $T = 50$  K for XPS and XAS, respectively. The overall energy resolution was approximately 1.0 eV and 0.7 eV for XPS and XAS, respectively. Throughout the photoemission measurements, energies were carefully calibrated using gold evaporated on the sample surface just after each series of measurements.

## III. RESULTS

### A. Chemical potential shift

Valence-band spectra of  $\text{La}_{1.17-x}\text{Pb}_x\text{VS}_{3.17}$  are shown in Fig. 1. The broad band around  $\sim -4$  eV and the peak at  $\sim -0.5$  eV are mainly derived from the S 3*p* and V 3*d* orbitals, respectively. The spectral weight at  $\mu$  is depressed at  $T = 14$  K for all the compositions including the metallic samples, although there should be no energy gap nor a pseudogap in the V 3*d* band according to the local-density-approximation (LDA) band-structure calculation of the parent material  $\text{VS}_2$ .<sup>16</sup>

The energy shift of the S 3*p* band can be accurately determined from the valence-band spectra, because we find that the spectral shape of the S 3*p* band remains virtually unchanged except for a rigid energy shift with Pb substitution  $x$ . Although it appears that the intensity of the secondary background slightly changes with samples in the lower kinetic-energy region ( $E < -5$  eV), the secondary background hardly affects the spectra in the higher kinetic-energy region ( $E > -4$  eV). Figures 2(a) and 2(b) show that the spectra of the leading edge of the S 3*p* peak have almost identical curve in a wide energy range for all the compositions. Therefore, we have determined the S 3*p* shift from the energy shift of the leading-edge midpoint of the S 3*p* peak, as shown in Fig. 2(c).

The rigid-band-like shift of the S 3*p* band is most likely due to the shift of the chemical potential  $\mu$  with carrier doping. In order to confirm this, the energy shifts of the core levels have been measured as in the previous studies on other filling-controlled materials.<sup>17,18,19,20,21</sup> As shown in Fig. 3, the La, Pb, and S core levels follow the shift of the S 3*p* valence band within experimental uncertainties. On the other hand, the V core level is shifted in the opposite direction, i.e., towards higher binding energies with hole doping. This shift is caused by the ex-

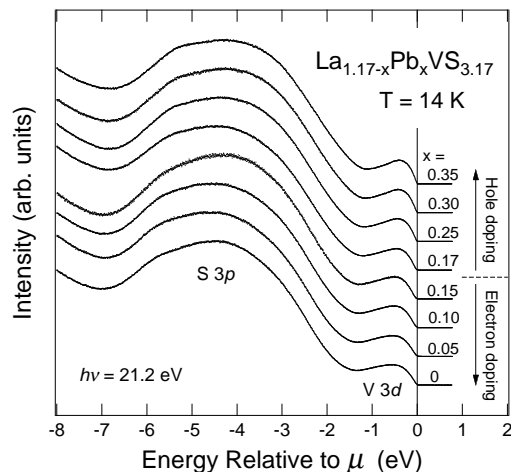


FIG. 1: Valence-band spectra of  $\text{La}_{1.17-x}\text{Pb}_x\text{VS}_{3.17}$ , taken at  $T = 14$  K using the He I resonance line ( $h\nu = 21.2$  eV). Spectral weight near  $\mu$  is depressed for all the compositions.

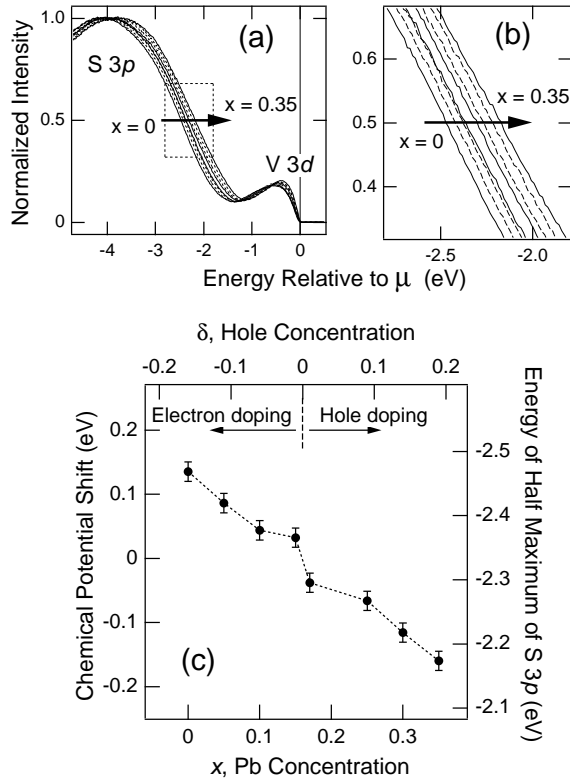


FIG. 2: Energy shift of the S 3p valence band. (a) Valence-band spectra normalized to the maximum spectral intensity around  $-4$  eV. Secondary backgrounds have been subtracted from the spectra. The leading edge of the S 3p band is rigidly shifted with Pb concentration  $x$ . (b) Enlarged view of the valence-band spectra around the leading-edge midpoint of the S 3p band. (c) Chemical-potential shift deduced from the energy shift of the leading edge of the S 3p band as a function of  $x$ . The energy shift shows a jump between the electron- and hole-doped sides.

tra contributions from the varying number of transition-metal  $d$  electrons, so-called chemical shift, as in the cases of the other filling-controlled materials.<sup>17,18,19,20,21</sup> As shown by the plot at the bottom of Fig. 3, the energy difference between V 2p and S 3p, ( $E_{V\ 2p} - E_{S\ 3p}$ ) shows nearly linear dependence on  $x$ . Therefore, the observed V 2p shift is decomposed into two components: one is the shift which is linear in  $x$  and the other is the shift which is common to all the core levels and the valence band. The former shift is proportional to the V valence and the latter common shift should reflect the shift of the chemical potential. Here, the changes in the Madelung potential upon substituting Pb for La does not account for the experimental result, because they should be different between the different atomic sites, particularly between the cations and anions. The present result is remarkably similar to the cases of the other filling-controlled systems in that all the core levels except for the core level of the transition-metal element are shifted by the same amount owing to the chemical-potential shift.<sup>17,18,19,20,21</sup>

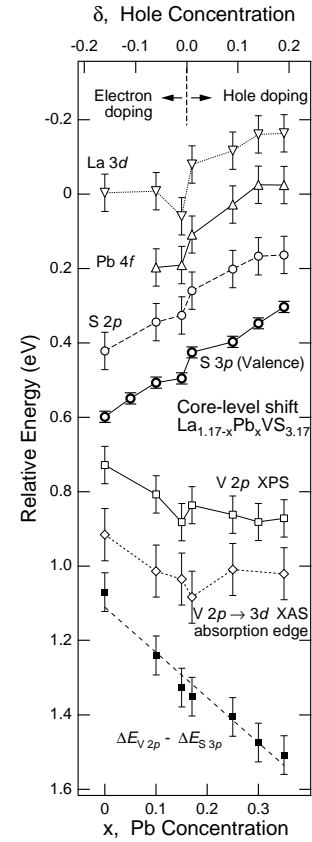


FIG. 3: Energy shifts of the La 3d, Pb 4f, S 2p, and V 3d core levels. The energy shift of the V 2p  $\rightarrow$  3d x-ray absorption edge is also shown.

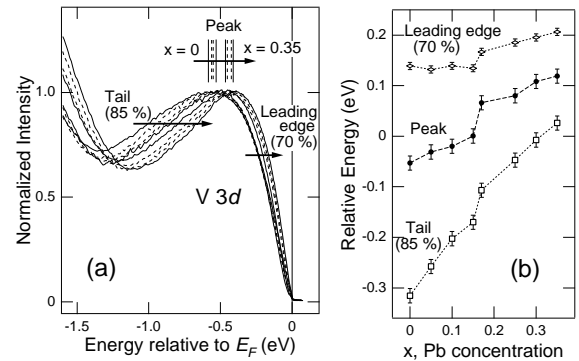


FIG. 4: Energy shift of the V 3d band. (a) Spectra of the V 3d band normalized to the maximum spectral intensity at the V 3d band peak. The energy shifts of the leading edge and tail of the V 3d band are determined, respectively, by the 70% and 85% level of the V 3d maximum intensity around  $-0.5$  eV. (b) Energy shifts of the leading edge, the peak, and the tail of the V 3d band. While the spectral shape of V 3d band gradually changes with  $x$ , a discontinuous energy shift has also been observed for V 3d between  $x = 0.15$  and  $0.17$ .

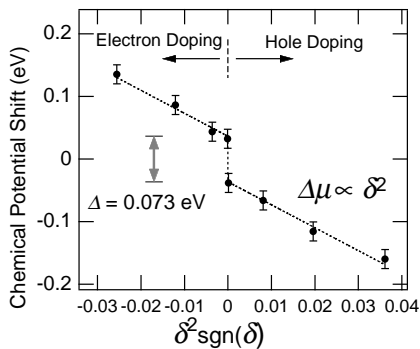


FIG. 5: Chemical-potential shift as a function of the square of the hole concentration,  $\delta^2 \text{sgn}(\delta)$ , showing a behavior as  $\Delta\mu \propto \delta^2$ .

Thus, we identify the energy shift of the S  $3p$  valence band shown in Fig. 2(c) as representing the chemical-potential shift. Then, one may find that the chemical potential is abruptly shifted by  $\sim 0.07$  eV between  $x = 0.15$  and  $0.17$ . It is difficult to use the V  $3d$  band as a direct measure of the chemical-potential shift, because the spectral shape of the V  $3d$  have large  $x$ -dependence. Nevertheless, a discontinuity has also been observed in the energy shifts of the leading edge, peak and tail of the V  $3d$  band, as shown in Fig. 4. Therefore, we concluded that the shift of the chemical potential jumps between  $x = 0.15$  and  $0.17$ , i.e., across the Mott insulating state. This suggests that an energy gap is opened when  $x \sim 0.16$  or when the filling of the V  $3d$  band becomes 2 and that the magnitude of the gap is  $\sim 0.07$  eV. When a sufficient number of carriers are doped, namely, in the overdoped region  $|\delta| \gtrsim 0.1$  the chemical potential  $\mu$  is monotonously shifted as in a normal metal on both the electron- and hole-doped sides. In the underdoped region, on other hand, the shift of the chemical potential is deviated from the monotonic behavior and seems to be suppressed towards the insulator limit. Since the spectral weight decreases towards  $\mu$ , the observed suppression of the chemical-potential shift is inconsistent with the rigid band picture of the conventional band insulator, but in good agreement with  $\Delta\mu \propto \delta^2$ , which has been predicted for the two-dimensional Hubbard model,<sup>22</sup> as shown by dotted lines in Fig. 5.

### B. Doping dependence of the electronic structure

The doping dependence of the V  $3d$  valence-band spectra has been investigated at low temperature  $T = 14$  K. The result is shown in Figs. 6 and 7. The V  $3d$  band shows a general trend of being shifted towards  $\mu$  with substitution of Pb for La. Since the spectral intensity at  $\mu$  always remains low, the total width of the V  $3d$  band becomes somewhat narrower with increasing  $x$ . It should be noted that between  $x = 0.15$  and  $0.17$ , the higher binding-energy side of the V  $3d$  band is rigidly

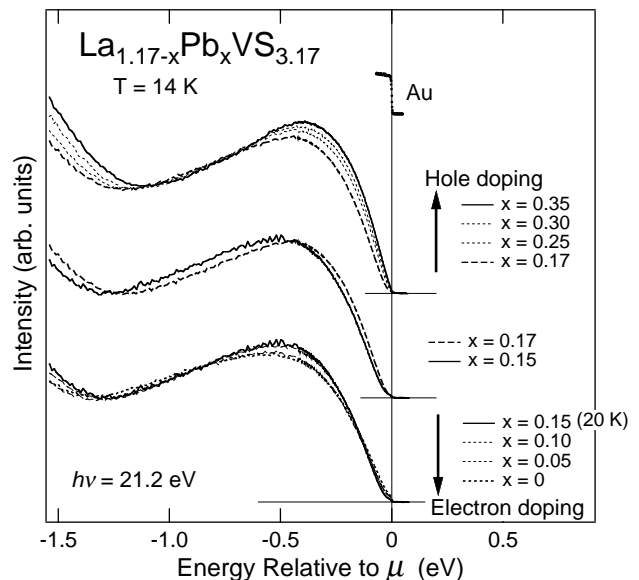


FIG. 6: Doping dependence of the V  $3d$  valence-band spectra taken at  $T = 14$  K. The samples  $x = 0.17$  and  $0.15$  are slightly hole- and electron-doped, respectively, and show a rather large difference in spite of the small difference in  $x$ .

shifted by a large amount in spite of the small change in  $x$ , implying that the chemical potential jumps across the gap between the electron- and hole-doped samples, as described above.

Starting from the Mott insulator  $x \simeq 0.16$ , when the electrons are doped, a weak Fermi edge appears as shown in Fig. 7(a), and the spectral weight within  $\sim 0.1$  eV of  $\mu$  is increased at the cost of the decrease in the spectral weight around  $-0.5$  eV. This means that spectral-weight transfer occurs upon electron doping from  $\sim -0.5$  eV to near  $\mu$ . If one takes into account the upward chemical-potential shift by  $\sim 0.1$  eV from  $x = 0.15$  to  $x = 0$ , the spectral-weight transfer into the gap region should be considered even larger, as schematically illustrated in Fig. 8. When the holes are doped into the  $x \simeq 0.16$  Mott insulator, the spectral weight in the vicinity of  $\mu$  increases. However, the increase rate from  $x = 0.17$  to  $0.35$  is lower than that expected from the  $x = 0.17$  spectrum shifted according to the rigid-band model. This implies that spectral weight is depleted around  $\mu$  from what would be expected from the rigid-band model for all the compositions as a result of pseudogap formation, as illustrated in Fig. 8.

The spectral weight at  $\mu$ ,  $\varrho(\mu)$ , plotted in Fig. 7 (c) has been determined by integrating the spectral intensity in the energy range of  $E > 10$  meV. Although  $\varrho(\mu)$  is always small, it shows a clear doping dependence resembling the doping dependence of thermodynamic properties, as shown in Fig. 7 (c). Here, the spectral intensities for the different compositions have been normalized to the maximum intensity of the S  $3p$  band. Corresponding to the fact that the electrical resistivity shows the transition to the insulator in the vicinity of  $x \simeq 0.16$ ,<sup>10,11,12</sup>

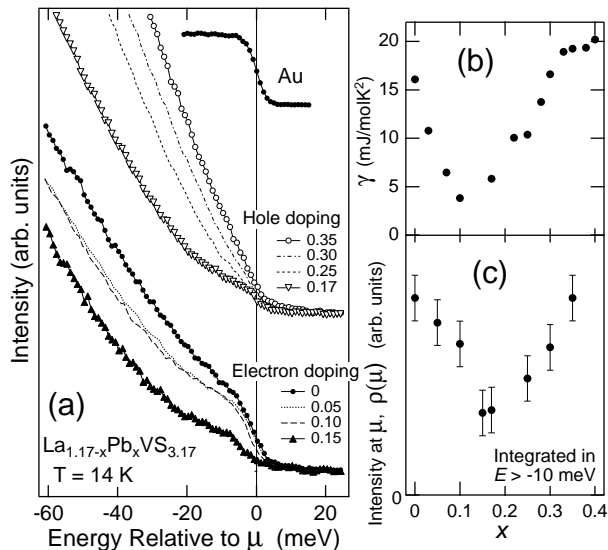


FIG. 7: (a) Doping dependence of photoemission spectra around  $\mu$  taken at  $T = 14$  K. The spectral intensities for the different compositions have been normalized to the maximum intensity of the S  $3p$  band. The gold Fermi edge is also shown. (b) Doping dependence of the low-temperature electronic specific-heat coefficient  $\gamma$ , taken from Ref. 12. (c) Doping dependence of the photoemission intensity at  $\mu$ ,  $\rho(\mu)$ , approximately determined by integrating spectral intensity in the energy range of  $E > -10$  meV.

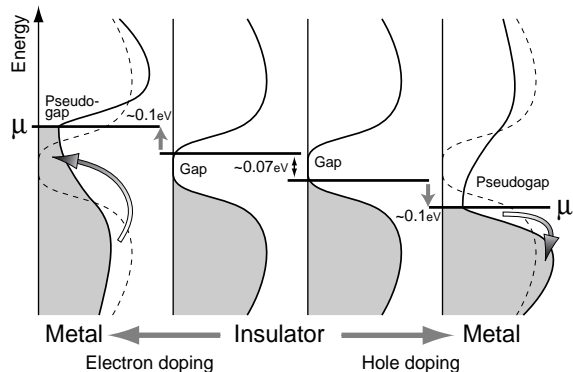


FIG. 8: Schematic picture illustrating the evolution of the low-energy electronic structure with carrier doping. The dashed curves are the spectrum of the insulator.

$\rho(\mu)$  decreases as  $x \rightarrow 0.16$ , i.e., as the carrier density decreases either from the electron-doped side or the hole-doped side. Figures 7(b) and 7(c) show that the doping dependence of  $\rho(\mu)$  is similar to that of the low-temperature electronic specific-heat coefficient  $\gamma$ ,<sup>12</sup> which is proportional to the QP density at  $\mu$ ,  $N^*(\mu)$ . The doping dependence of  $\gamma$  indicates that no enhancement in the electron effective mass  $m^*$  occurs near the metal-to-insulator transition in the present system. Alternatively, the present photoemission results suggest that transition to the insulator is caused by the reduction of the effective

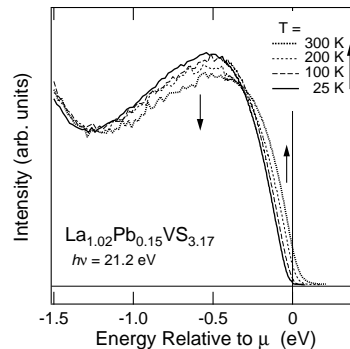


FIG. 9: Temperature dependence of the V  $3d$  valence-band spectrum for  $x = 0.15$ . As the temperature increases, the spectral weight around  $\mu$  increases, while the spectral weight around the V  $3d$  peak position is reduced.

carrier number due to the pseudogap formation.<sup>23</sup>

### C. Temperature dependence of the electronic structure

Next, the temperature dependence of the gap and the pseudogap in  $\text{La}_{1.17-x}\text{Pb}_x\text{VS}_{3.17}$  was investigated. The result for the insulating sample  $x = 0.15$  is shown in Fig. 9. As the temperature increases, dramatic spectral weight transfer occurs as shown in the figure: the intensity around  $\mu$  ( $E \gtrsim -0.3$  eV) increases, while the peak intensity of the V  $3d$  band ( $-1.2 \lesssim E \lesssim -0.4$  eV) decreases. Here, the energy scale corresponding to the temperature change ( $4k_B T \lesssim 0.1$  eV) is of the order of the energy gap  $\sim 0.06$  eV, while the spectral weight transfer occurs over a much wider energy range ( $\sim 1$  eV), as have been observed in many strongly correlated systems. In order to eliminate the effect of the temperature dependence of the Fermi-Dirac distribution function and to extract the intrinsic temperature dependence of the pseudogap line shape,<sup>24,25</sup> the spectra have been divided by the Fermi-Dirac distribution function, as shown in Fig. 10(b). The figure clearly shows that the gap of the insulating  $x = 0.15$  sample is rapidly filled with temperature. The increase of the spectral weight at  $\mu$  is continuous and monotonic at least from  $T = 14$  K to 300 K, and shows no anomaly at  $T \simeq 280$  K unlike the thermal dilatation and the ultrasound velocity. Figure 11 schematically illustrates the evolution of the electronic structure with increasing temperature.

In Fig. 10, temperature-dependent spectra are also shown for several different composition. It should be noted that the gap filling with temperature looks quite similar for all the compositions, and does not depend on whether it has a real gap or a pseudogap. At room temperature 300 K, the spectral intensity at  $\mu$  is filled up to about half of the peak intensity of the V  $3d$  band, so that the spectra at 300 K appear almost those of a

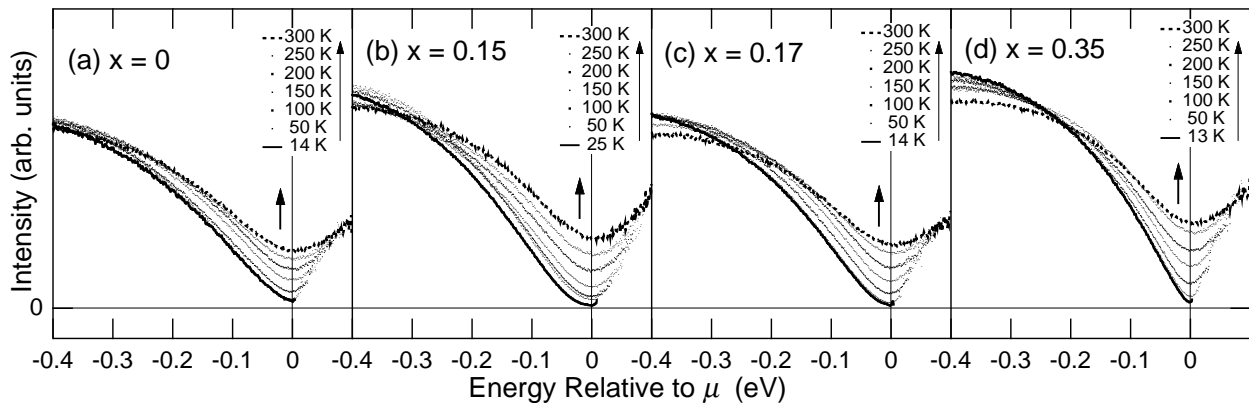


FIG. 10: Temperature dependence of the photoemission spectra around  $\mu$ , divided by the Fermi-Dirac distribution function for  $x = 0, 0.15, 0.17$ , and  $0.35$ . It is clearly shown that the gap or the pseudogap is rapidly filled with increasing temperature.

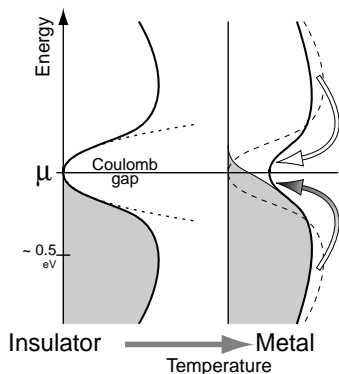


FIG. 11: Schematic picture illustrating the evolution of the electronic structure with increasing temperature for an insulating sample.

normal metal.

#### IV. DISCUSSION

Now, we discuss on the nature of the metal-to-insulator transition in  $\text{La}_{1.17-x}\text{Pb}_x\text{VS}_{3.17}$ . Since the three  $t_{2g}$  orbitals of the V  $3d$  states are thought to be nearly degenerate, the insulating state around  $x \simeq 0.16$  is difficult to be understood as a conventional band insulator, and should be explained as a Mott insulator induced by the repulsive electron-electron interaction. In fact, the observed critical behavior of the chemical-potential shift around MIT is consistent with the Mott-Hubbard model calculation. Then, the nonmagnetic behavior of the insulating state of  $\text{La}_{1.17-x}\text{Pb}_x\text{VS}_{3.17}$  at low temperatures would be interpreted as due to a singlet formation out of the atomic  $S = 1$  state of the  $d^2$  configuration, e.g., the formation of a small cluster such as  $V_3$  trimer.<sup>13</sup> In the case of the weak interaction limit, such a picture of the insulating state becomes that of a charge-density-wave (CDW) insulator. Whether the interaction is strong or weak, these

insulating states require lattice distortion, which is indeed observed as the anomaly in the thermal dilatation and in the ultrasound velocity at  $T \simeq 280$  K.<sup>12</sup>

Although the chemical-potential shift and the transport properties indicate that the Mott MIT occurs, no effective mass enhancement has been observed near the MIT of  $\text{La}_{1.17-x}\text{Pb}_x\text{VS}_{3.17}$  in the electronic specific-heat coefficient  $\gamma$  nor in the photoemission spectral weight at  $\mu$ ,  $\rho(\mu)$ . Alternatively,  $\rho(\mu)$  is decreased towards the insulating phase because the pseudogap develops at  $\mu$ . With increasing temperature, the pseudogap is rapidly filled. The behaviors of both the chemical-potential shift and the doping and temperature dependence of  $\rho(\mu)$  are similar to those of the high- $T_c$  cuprate  $\text{La}_{2-x}\text{Sr}_x\text{CuO}_4$ ,<sup>7,26</sup> rather than those of the three-dimensional typical Mott MIT system  $\text{La}_{1-x}\text{Sr}_x\text{TiO}_3$ .<sup>4,5</sup> Therefore, the present results suggest that the dimensionality of the system is crucial to whether the mass enhancement occurs or the pseudogap behavior is observed. Then, we consider a possible origin of the suppression of  $\rho(\mu)$  near MIT. For  $\text{La}_{2-x}\text{Sr}_x\text{CuO}_4$ , the formation of the large pseudogap is closely related to the antiferromagnetic correlation<sup>7</sup> or singlet correlation.<sup>27</sup> Thus, a singlet formation of the  $V_3$  trimer may lead to the disappearance of the electronic states around  $\mu$ . A Hubbard model calculation has shown that dimerization may reconcile the suppression of the chemical-potential shift with the absence of the mass enhancement.<sup>23</sup>

In addition, the effect of structural disorder cannot be ignored in the filling-controlled systems. In particular, for the present system, the parent insulator  $\text{La}_{1.01}\text{Pb}_{0.16}\text{VS}_{3.17}$  is nonstoichiometric unlike the stoichiometric  $\text{La}_2\text{CuO}_4$ .<sup>28</sup> (Scraping sample surfaces may also introduces additional disorder for the present experiment.) When the carrier concentration is low, random potential leads to Anderson localization. Doped carriers just being localized are more strongly affected by the long-range Coulomb interaction between electrons, and a so-called ‘‘Coulomb gap’’ is formed at  $\mu$ . Efros and Shklovskii theoretically predicted that

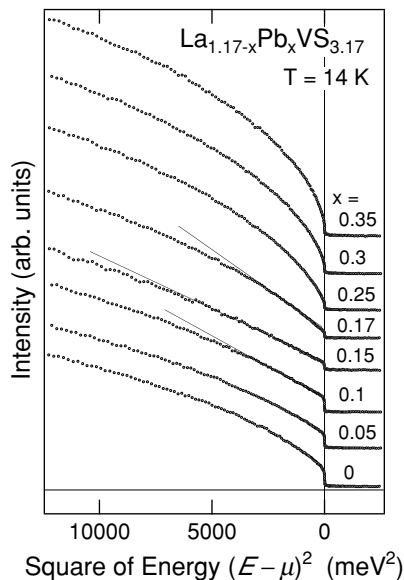


FIG. 12: Photoemission spectra near  $\mu$  taken at  $T = 14$  K, plotted against the square of binding energy. The spectrum for  $x = 0.15$  has the widest straight portion near  $\mu$ .

long-range Coulomb interaction in a disordered insulator drives the electronic states around  $\mu$  to form a soft gap:  $N(E)/N_0(\mu) = |(E - \mu)/\Delta_C|^2$ , where  $N_0(\mu)$  is non-interacting DOS at  $\mu$ .<sup>29</sup> Such a Coulomb gap has also been observed in the photoemission spectra of  $\text{Fe}_3\text{O}_4$  and  $\text{Ti}_4\text{O}_7$ .<sup>30,31</sup> As seen from Figs. 9 and 10, the leading edge of the V 3d band is broadened and obscured for all the compositions. In particular, for the insulating samples  $x = 0.15$  and 0.17, the spectral intensity appears parabolic near  $\mu$ ,  $\rho(E) \propto (E - \mu)^2$  at low temperatures, as shown in Fig. 10. In order to see this more clearly, the spectra at low temperatures are plotted as a function of the square of energy in Fig. 12. While the spectra for both metallic ends  $x = 0$  and 0.35 are convex near  $\mu$ , the spectrum of the most insulating sample  $x = 0.15$  shows a straight portion over a wide energy range below  $\mu$ , suggesting the formation of a Coulomb gap. A small residual step at  $\mu$  for  $x = 0.15$  indicates that the Coulomb-gap opening is incomplete, but it is difficult at present to judge whether this is an intrinsic feature of the material or is due to small residual metallic regions in the sample. The spectral evolution from the pseudogap to the Coulomb gap with decreasing carrier concentration is quite similar to that observed for  $\text{Fe}_3\text{O}_4$  and  $\text{Ti}_4\text{O}_7$ .<sup>30,31</sup> In order to estimate the magnitude of  $\Delta_C$ , we simply assume that the noninteracting DOS,  $N_0(\mu)$ , is

given by the DOS of the band calculation of  $\text{VS}_2$ .<sup>16</sup> Then we obtain  $\sim 0.15$  eV as an upper limit of  $\Delta_C$ . Therefore,  $\Delta_C$  appears comparable to the Mott insulating gap  $\sim 0.07$  eV. The observed photoemission spectra suggest that the long-range Coulomb interaction has impact on the electronic states around  $\mu$ , and that the structural disorder is important in the  $\text{La}_{1.17-x}\text{Pb}_x\text{VS}_{3.17}$  system.

## V. CONCLUSION

In conclusion, photoemission experiments have revealed the evolution of the electronic structure across the filling-controlled MIT in the misfit-layer  $\text{La}_{1.17-x}\text{Pb}_x\text{VS}_{3.17}$  system. The jump of the chemical potential between  $x = 0.15$  and 0.17 indicates the opening of a charge gap of  $\sim 0.07$  eV. The characteristic behavior of the chemical potential shift is consistent with the picture that the Mott MIT occurs in the present system as suggested from the transport properties. When hole or electron carriers are doped into the Mott insulator, the gap is filled while spectral weight at  $\mu$ ,  $\rho(\mu)$ , is suppressed for all the compositions due to the pseudogap formation. With increasing temperature, the gap is rapidly filled up and  $\rho(\mu)$  increases monotonously. On approaching the MIT from the metallic side,  $\rho(\mu)$  decreases, indicating that the effective carrier number vanishes towards the insulating phase, consistent with the decrease of the specific-heat coefficient.  $\text{La}_{1.17-x}\text{Pb}_x\text{VS}_{3.17}$  is another two-dimensional filling-controlled MIT system which shows anomalous behaviors similar to the high- $T_c$  cuprate  $\text{La}_{2-x}\text{Sr}_x\text{CuO}_4$  in the chemical potential shift and the doping and temperature dependence of  $\rho(\mu)$ . The present result implies the importance of the two-dimensionality in the metal-insulator transition. The observed Coulomb-gap behavior is attributed to the impact of long-range Coulomb interaction on the Anderson localized carriers. The present result shows that one should consider the effect of structural disorder, which is intricately involved to the filling-controlled MIT, in addition to electron correlation.

## ACKNOWLEDGMENTS

This work was partly supported by a Grant-in Aid for Research in Priority Area ‘‘Novel Quantum Phenomena in Transition-Metal Oxides’’ from the Ministry of Education, Culture, Sports, Science and Technology, Japan. Part of this work has been done under the approval of the Program Advisory Committee of Photon Factory (PAC-94G361).

\* Present address: Graduate School of Science, Hiroshima University, Higashi-Hiroshima 739-8526, Japan.

<sup>1</sup> M. Imada, A. Fujimori, and Y. Tokura, Rev. Mod. Phys. **70**, 1039 (1998).

<sup>2</sup> A. Fujimori, J. Phys. Chem. Solids **53**, 1595 (1992).

<sup>3</sup> T. Katsufuji, Y. Taguchi, and Y. Tokura, Phys. Rev. B **56**, 10145 (1997).

<sup>4</sup> K. Kumagai, T. Suzuki, Y. Taguchi, Y. Okada, Y. Fu-

- jishima, and Y. Tokura, Phys. Rev. B **48**, 7636 (1993).
- <sup>5</sup> T. Yoshida, A. Ino, T. Mizokawa, A. Fujimori, Y. Taguchi, T. Katsufuji, and Y. Tokura, Europhys. Lett. **59**, 258 (2002).
  - <sup>6</sup> A. Georges, G. Kotliar, W. Krauth, and M. J. Rozenberg, Rev. Mod. Phys. **68**, 13 (1996).
  - <sup>7</sup> A. Ino, T. Mizokawa, K. Kobayashi, A. Fujimori, T. Sasagawa, T. Kimura, K. Kishio, K. Tamasaku, H. Eisaki, and S. Uchida, Phys. Rev. Lett. **81**, 2124 (1998).
  - <sup>8</sup> N. Momono, M. Ido, T. Nakano, M. Oda, Y. Okajima, and K. Yamaya, Physica C **233**, 395 (1994).
  - <sup>9</sup> Effects of disorder has been most dramatically demonstrated in  $\text{LaNi}_{1-x}\text{Mn}_x\text{O}_3$  and  $\text{LaNi}_{1-x}\text{Fe}_x\text{O}_3$ . [D. D. Sarma, A. Chainani, S. R. Krishnakumar, E. Vescovo, C. Carbone, W. Eberhardt, O. Rader, Ch. Jung, Ch. Hellwig, W. Gudat, H. Srikanth, and A. K. Raychaudhuri, Phys. Rev. Lett **80**, 4004 (1998).]
  - <sup>10</sup> T. Nishikawa, Y. Yasui, and M. Sato, J. Phys. Soc. Jpn. **63**, 3218 (1994).
  - <sup>11</sup> Y. Yasui, T. Nishikawa, Y. Kobayashi, M. Sato, T. Nishiooka, and M. Kotani, J. Phys. Soc. Jpn. **64**, 3890 (1995).
  - <sup>12</sup> T. Nishikawa, Y. Yasui, Y. Kobayashi, and M. Sato, J. Phys. Soc. Jpn. **65**, 2543 (1996).
  - <sup>13</sup> Y. Kobayashi, M. Kasai, Y. Yasui, T. Nishikawa, and M. Sato, J. Phys. Soc. Jpn. **66**, 4027 (1997).
  - <sup>14</sup> G. A. Wiegers, A. Meetsma, S. van Smaalen, R. J. Haange, J. Wulff, T. Zeinstra, J. L. de Boer, S. Kuypers, G. Van Tendeloo, J. Van Landuyt, S. Amelinckx, A. Meerschaut, P. Rabu, and J. Rouxel, Solid State Commun. **70**, 409 (1989).
  - <sup>15</sup> R. J. Cava, B. Batlogg, R. B. van Dover, A. P. Ramirez, J. J. Krajewski, W. F. Peck, Jr., and L. W. Rupp, Jr., Phys. Rev. B **49**, 6343 (1994).
  - <sup>16</sup> H. W. Myron, Physica B & C **99**, 243 (1980); For the sake of comparison, the calculation of  $\text{VS}_2$  is shifted as in the rigid-band model, so that the filling of  $3d$  band is corrected to that of  $\text{La}_{1.17-x}\text{Pb}_x\text{VS}_{3.17}$ .
  - <sup>17</sup> A. Ino, T. Mizokawa, A. Fujimori, K. Tamasaku, H. Eisaki, S. Uchida, T. Kimura, T. Sasagawa, and K. Kishio, Phys. Rev. Lett. **79**, 2101 (1997).
  - <sup>18</sup> N. Harima, J. Matsuno, A. Fujimori, Y. Onose, Y. Taguchi, and Y. Tokura, Phys. Rev. B **64**, 220507 (2001).
  - <sup>19</sup> M. Satake, K. Kobayashi, T. Mizokawa, A. Fujimori, T. Tanabe, T. Katsufuji, and Y. Tokura, Phys. Rev. B **61**, 15515 (2000).
  - <sup>20</sup> K. Kobayashi, T. Mizokawa, A. Ino, J. Matsuno, A. Fujimori, H. Samata, A. Mishiro, Y. Nagata, and F. M. F. de Groot, Phys. Rev. B **59**, 15100 (1999).
  - <sup>21</sup> A. Fujimori, A. Ino, J. Matsuno, T. Yoshida, K. Tanaka, and T. Mizokawa, J. Electron Spectrosc. Relat. Phenom. **124**, 127 (2002).
  - <sup>22</sup> N. Furukawa and M. Imada, J. Phys. Soc. Jpn. **64**, 2557 (1993).
  - <sup>23</sup> M. Imada, J. Phys. Soc. Jpn. **62**, 1105 (1993).
  - <sup>24</sup> T. Susaki, T. Mizokawa, A. Fujimori, A. Ohno, T. Tonogai, and H. Takagi, Phys. Rev. B **58**, 1197 (1998).
  - <sup>25</sup> T. Greber, T. J. Kreuzt, and J. Osterwalder, Phys. Rev. Lett. **79**, 4465 (1997).
  - <sup>26</sup> T. Sato, T. Yokoya, Y. Naitoh, T. Takahashi, K. Yamada, and Y. Endoh, Phys. Rev. Lett. **83**, 2254 (1999).
  - <sup>27</sup> T. Nishikawa, J. Takeda, and M. Sato, J. Phys. Soc. Jpn. **62**, 2568 (1993).
  - <sup>28</sup> In addition to the substitution of Pb for La, the mismatch of the lattice periodicity between the  $\text{VS}_2$  and LaS layers may induce effects similar to the “random potential” on electrons in the  $\text{VS}_2$  layer.
  - <sup>29</sup> A. L. Efros and B. I. Shklovskii, J. Phys. C **8**, L49 (1975).
  - <sup>30</sup> A. Chainani, T. Yokoya, T. Morimoto, T. Takahashi, and S. Todo, Phys. Rev. B **51**, 17976 (1995).
  - <sup>31</sup> K. Kobayashi, T. Susaki, A. Fujimori, T. Tonogai, and H. Takagi, Europhys. Lett. **56**, 868 (2002).